



# HHS Public Access

Author manuscript

*Biochemistry*. Author manuscript; available in PMC 2021 July 07.

Published in final edited form as:

*Biochemistry*. 2020 July 07; 59(26): 2468–2478. doi:10.1021/acs.biochem.0c00359.

## Metal Sequestration and Antimicrobial Activity of Human Calprotectin are pH-Dependent

Tomer Rosen, Elizabeth M. Nolan\*

Department of Chemistry, Massachusetts Institute of Technology, 77 Massachusetts Avenue, Cambridge, MA 02139, USA

### Abstract

Human calprotectin (CP, S100A8/S100A9 oligomer) is an abundant innate immune protein that sequesters transition metal ions in the extracellular space to limit nutrient availability and the growth of invading microbial pathogens. Our current understanding of the metal-sequestering ability of CP is based on biochemical and functional studies performed at neutral or near-neutral pH. Nevertheless, CP can be present throughout the human body and is highly expressed at infection and inflammation sites that tend to be acidic. Here, we evaluate the metal-binding and antimicrobial properties of CP in the pH 5.0–7.0 range. We show that Ca(II)-induced tetramerization, an important process for the extracellular functions of CP, is perturbed by acidic conditions. Moreover, low pH impairs the antimicrobial activity of CP against some bacterial pathogens, including *Staphylococcus aureus* and *Salmonella enterica* serovar Typhimurium. At mildly acidic pH, CP loses the ability to deplete Mn from microbial growth medium, indicating that Mn(II) sequestration is attenuated under acidic conditions. Evaluation of the Mn(II)-binding properties of CP at pH 5.0–7.0 indicate that mildly acidic conditions lower the Mn(II)-binding affinity of the His<sub>6</sub> site. Lastly, CP is less effective at preventing capture of Mn(II) by the bacterial solute-binding proteins MntC and PsaA at low pH. These results indicate that acidic conditions compromise the ability CP to sequester Mn(II) and thereby starve microbial pathogens of this nutrient. Broadly, this work highlights the importance of considering the chemical complexity of biological sites when describing the interplay between CP and microbes in host-pathogen interactions.

### Graphical Abstract

---

\*Corresponding author: Inolan@mit.edu, Phone: 617-452-2495.

Supporting Information

Complete experimental methods, Tables S1–S7, Figures S1–S15, and supporting references. This material is available free of charge via the Internet at <http://pubs.acs.org>.

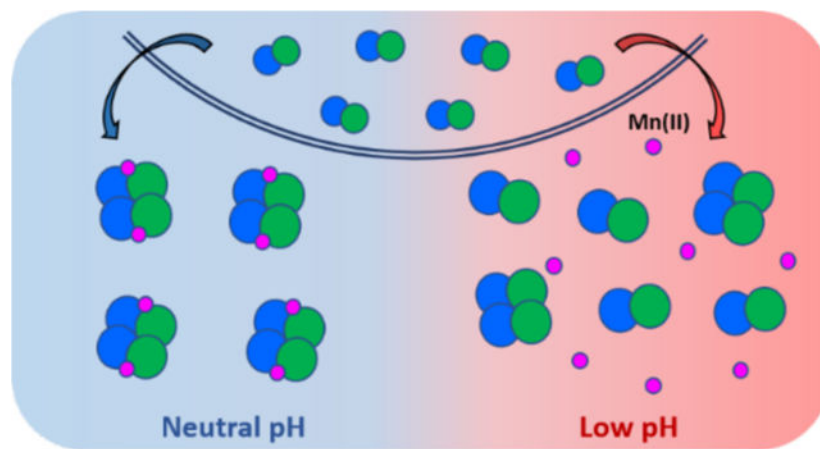
Accession Codes

Human (*Homo sapiens*) S100A8, Uniprot: P05109

Human (*Homo sapiens*) S100A9, Uniprot: P06702

*Streptococcus pneumoniae* D39 PsaA, Uniprot: P0A4G2

*Staphylococcus aureus* MntC, Uniprot: Q8VQS9



## Introduction

Microbial pathogens face host environments during colonization and infection that pose significant stress conditions, influencing microbial growth and survival. Host limitation of nutrients, including essential transition metals (e.g. Mn, Fe, Zn), in a process termed “nutritional immunity” creates challenges for invading microbes and is an important host-defense mechanism against pathogens.<sup>1, 2</sup> As part of the innate immune response, a variety of host cells deploy metal-chelating proteins to withhold metal nutrients and thereby starve pathogens during the early stages of infection.<sup>1</sup> The human S100 protein calprotectin (CP, S100A8/S100A9 oligomer, MRP8/MRP14 oligomer, calgranulin A/B oligomer) is an abundant antimicrobial protein that is produced by several types of white blood cells and epithelial cells.<sup>3, 4</sup> Upon release to the extracellular environment, CP limits microbial growth by sequestering bioavailable transition metal ions.<sup>5–12</sup>

Extensive biophysical and biochemical studies have provided important insights into the molecular basis of metal withholding by human CP.<sup>12</sup> The protein exists as a heterooligomer of the S100 proteins S100A8 ( $\alpha$  subunit) and S100A9 ( $\beta$  subunit) (Figure 1).<sup>13–16</sup> Each subunit possess two EF-hand Ca(II)-binding domains. In the absence of Ca(II), apo CP exists as a heterodimer ( $\alpha\beta$ ), and Ca(II) binding promotes self-oligomerization into a heterotetrameric complex ( $\alpha_2\beta_2$ ).<sup>13–16</sup> Two additional sites for transition metal binding are located at the S100A8/S100A9 heterodimer interface. Site 1 is a His<sub>3</sub>Asp motif that coordinates Zn(II) with high affinity, and site 2 is a functionally versatile His<sub>6</sub> motif that binds Mn(II), Fe(II), Ni(II), and Zn(II) with high affinity.<sup>8–11, 17, 18</sup> Recent work has shown that CP can also sequester Cu, but the details of this behavior are unclear.<sup>19</sup> In the current working model, the high extracellular Ca(II) concentration acts as an environmental cue that promotes heterotetramer formation, leading to enhanced transition metal ion affinities, antimicrobial activity and protease stability.<sup>8, 12, 20</sup>

This working model has been proposed based on many studies of CP largely conducted at neutral or near-neutral pH. Although these conditions are physiologically relevant, other pH regimes exist *in vivo* and are encountered by host-defense factors and pathogens. Under normal conditions, acidic environments occur in the gastrointestinal and genital tracts, skin

and intracellular endocytic vesicles.<sup>22–25</sup> Moreover, various infection and inflammation sites are associated with acidic pH regimes, including airways in the cystic fibrosis (CF) lung and the gut during inflammatory bowel disease (IBD).<sup>22, 26</sup>

Microbes have evolved mechanisms to sense and initiate appropriate responses that allow survival and growth in acidic environments.<sup>27</sup> These acid tolerance response (ATR) systems have been characterized in commensal and pathogenic microbes, including *Lactobacillus* spp.,<sup>28, 29</sup> *Escherichia coli*,<sup>30</sup> *Salmonella enterica* serovar Typhimurium,<sup>31, 32</sup> *Helicobacter pylori*,<sup>33, 34</sup> *Klebsiella pneumoniae*,<sup>35</sup> *Staphylococcus aureus*,<sup>36, 37</sup> *Listeria monocytogenes*,<sup>38</sup> and *Candida albicans*.<sup>39</sup> Extracellular pH may also affect bacterial metal acquisition and homeostasis, for example, by prioritizing proton-driven metal transporters<sup>40</sup> or causing a shift from Fe(III) to Fe(II) uptake.<sup>41</sup> Such metal acquisition systems have been described as important for survival and as virulence factors for various pathogens that colonize acidic host compartments.<sup>42–46</sup>

Likewise, pH can affect the behavior of host-defense factors. Several studies demonstrated that low pH can attenuate or enhance antimicrobial activity and, in some cases, alter mechanism.<sup>47–50</sup> The airway surface liquid (ASL), a thin layer of fluid and mucus covering the surface of the airway epithelium, contains multiple antimicrobial factors.<sup>51</sup> In a CF pig model, the acidified ASL exhibited lower antimicrobial activity, presumably due to deactivation of ASL antimicrobials by low pH.<sup>52</sup> Subsequent investigations revealed that acidic conditions alter the activities of various antimicrobial peptides in the ASL, such as  $\beta$ -defensin 3 and LL-37.<sup>48</sup> From the standpoint of metal withholding, the effect of low pH on Fe(III) binding by transferrin (TF) and lactoferrin (LF) has been studied extensively. The Fe(III) affinity of TF decreases as the pH is lowered from 7.4 to 5.5, resulting in Fe(III) release in acidic environments.<sup>53</sup> While this behavior is important for Fe delivery to host cells following TF endocytosis,<sup>54</sup> it has been suggested that some pathogens, including *S. aureus*, acidify the local environment to promote Fe(III) release from TF and thereby acquire this nutrient.<sup>55</sup> LF, in contrast, maintains its ability to bind and sequester Fe(III) at low pH.<sup>56</sup>

To the best of our knowledge, how acidic pH affects the biophysical and functional properties of CP has not been described. This information is important for conceptualizing how CP behaves in chemically diverse infection and inflammation sites. Indeed, CP can be present at many different environments, and previous work demonstrated that elevated levels of CP occur in the CF lung and IBD colon.<sup>57, 58</sup> The coordination chemistry of CP is complex and, in contemplating the consequences of acidic pH on metal binding by CP, the four Ca(II) binding EF-hand domains and the His<sub>6</sub> and His<sub>3</sub>Asp sites must be considered. In general terms, protonation of an ionizable ligand in a metal-binding site is expected to decrease the metal binding affinity at that site. The pK<sub>a</sub> values of the ionizable His and Asp metal-binding residues in CP are unknown, and these values can vary widely depending on their local environment in a protein.<sup>59, 60</sup> Nevertheless, we anticipated that the metal-binding properties of CP will vary with pH, hypothesizing that select residues in one or more of the metal-binding sites could become protonated at acidic pH. Indeed, protonation of His residues involved in Zn(II) binding was recently demonstrated for human S100A12, a host-defense protein that sequesters Zn(II) at two His<sub>3</sub>Asp sites, at mildly acidic pH.<sup>61</sup> Consequently, we reasoned that its metal-sequestering antimicrobial activity may be less

effective in acidic pH regimes. Alternatively, pH may influence protein structure, allostery, and the metal dependent self-association processes that afford the CP heterotetramer, which would presumably impact biological function.

In this work, we seek to expand the current working model for CP in the extracellular space and begin to integrate how low-pH regimes affect its biochemical properties and antimicrobial activity. We show that mildly acidic pH alters the metal-binding and antimicrobial activity of CP, rendering several bacterial species less susceptible to the protein. In particular, the ability of CP to sequester Mn(II) is markedly reduced in low pH regimes, suggesting that pathogens may benefit from acidic conditions to acquire Mn(II) from the host.

## Materials and Methods

Complete experimental details are provided as Supporting Information.

## Results

### Ca(II)-enhanced thermal stability is attenuated at low pH.

CP adopts a predominantly  $\alpha$ -helical secondary structure, a common feature of S100 proteins.<sup>13, 15</sup> Previous circular dichroism (CD) spectroscopy of CP and of the murine homolog mCP performed in the pH 7.5–8.5 range demonstrated that the presence Ca(II) ions and first-row transition metal ions has negligible effect on the secondary structure of these proteins.<sup>8, 10, 13, 62–64</sup> First, to evaluate whether lower pH perturbs the secondary structure of CP, we performed CD spectroscopy at pH 7.0 of CP and the S100A8(C42S)/S100A9(C3S) variant CP-Ser in the absence and presence of Ca(II) ions. CP-Ser exhibits similar metal-binding properties and antimicrobial activity to CP and has been routinely used in biochemical and functional studies.<sup>8–11, 13, 15, 17, 20, 65</sup> The CD spectra of CP and CP-Ser at pH 5.0–7.0 in the presence and absence of excess Ca(II) ions revealed that both proteins maintain their characteristic  $\alpha$ -helical secondary structures, defined by double minima at 208 and 222 nm (Figures 2A and S1–S2).

Prior thermal denaturation analyses of CP conducted at pH 7.5–8.5 demonstrated that Ca(II) binding increases stability to thermal denaturation.<sup>8, 64</sup> In agreement with this prior work, thermal denaturation of apo CP-Ser (10  $\mu$ M) at pH 7.0 afforded a melting temperature ( $T_m$ ) of 67 °C that increased to 83 °C when 2 mM Ca(II) was added to the protein solution (Figures 2B–C and S3–S4). A similar trend was observed when the assay was repeated at pH 6.0 and 5.5, affording  $T_m$  values of 66 and 64 °C for apo CP-Ser, and 80 and 77 °C for CP-Ser, respectively, in the presence of Ca(II). In contrast, Ca(II) supplementation had no effect on the  $T_m$  at pH 5.0, affording a similar  $T_m$  to apo CP-Ser ( $\approx$  66 °C), suggesting that Ca(II) binding to CP at low pH is impaired.

### Greater Ca(II) equivalents are required for complete tetramerization at low pH.

The thermal denaturation behavior of CP at low pH prompted us to investigate how pH affects the quaternary structure of CP and, in particular, the Ca(II)-dependent formation of heterotetramers. We employed analytical size-exclusion chromatography (SEC) to

investigate the oligomeric states of CP-Ser in the absence and presence of excess Ca(II) at pH 5.0–7.0 (Figures 3 and S5, Table S4). The elution volumes of apo CP-Ser (100  $\mu$ M) were similar across this pH range, spanning 11.5 mL to 11.9 mL at pH 7.0 and 5.0, respectively. These elution volumes correspond to a calculated molecular weight range of 30.1–28.5 kDa (Table S4), as expected for the heterodimer.<sup>8</sup> When 20 equivalents of Ca(II) were added to the samples and running buffers at pH 6.5–7.0, the elution volume of CP-Ser shifted to 10.7 mL (35.7 kDa), corresponding to the  $\alpha_2\beta_2$  form. This behavior is in agreement with our prior analytical SEC studies of CP-Ser at pH 7.0–7.5.<sup>8, 11, 20</sup> In contrast, higher equivalents of Ca(II) were required for CP-Ser to undergo complete tetramerization at pH < 6.5. At pH 6.0, full conversion to the heterotetramer form occurred in the presence of 50–100 equivalents of Ca(II), and in the pH 5.0–5.5 range, at least 100 equivalents of Ca(II) ions were required to reach an elution peak shift to 10.7 mL.

#### **Tetramerization is reversible at low pH.**

To ascertain whether low pH promotes the dissociation of Ca(II)-bound heterotetramers, we incubated CP-Ser (100  $\mu$ M) with Ca(II) (2 mM) at pH 7.0 to form heterotetramers, and then adjusted the pH to 5.5. Subsequent analytical SEC revealed a broad elution peak corresponding to a mixture of  $\alpha\beta$  and  $\alpha_2\beta_2$  species (Figure 4). Moreover, this peak sharpened and shifted to lower elution volumes upon addition of 20 or 100 equivalents of Ca(II) to the running buffer (Figure 4). Thus, acidic conditions promote heterotetramer dissociation, and the oligomeric state of CP at a given pH is unaffected by pre-existing quaternary structure. The broadened elution peaks at pH 5.5 suggest a dynamic tetramer-dimer equilibrium that is shifted to dimers at low pH. We previously reported a similar behavior for CP-Ser harboring oxidized methionine residues.<sup>65</sup>

#### **Antimicrobial activity of CP-Ser is attenuated at low pH.**

To evaluate the effect of low pH on the antimicrobial activity (AMA) of CP, we performed AMA assays against a selection of bacterial species that were reported to be susceptible to CP, have the capacity to cause human disease, and colonize acidic host compartments (Table S2).<sup>5–7, 9, 66–68</sup> These include the Gram-negative bacteria *E. coli* UTI89, *S. Typhimurium* IR715, *Pseudomonas aeruginosa* PAO1, *K. pneumoniae* ATCC 13883 and *Acinetobacter baumannii* ATCC 17961, and the Gram-positive bacterium *S. aureus* USA300 JE2. First, we evaluated the growth of these microbes at 37 °C in MES-buffered TSB medium (62:38 v/v MES:TSB) with the starting pH adjusted to 5.0–7.0. All cultures were supplemented with 2 mM Ca(II) to mimic extracellular Ca(II) levels. As expected, all six bacterial species grew under these conditions. Following 8 or 20 h of growth, *E. coli*, *S. Typhimurium*, *K. pneumoniae*, and *A. baumannii* grew to a similar OD<sub>600</sub> regardless of the initial pH of the medium (Figures 5 and S6). In contrast, *P. aeruginosa* cultured at an initial pH of 5.0 grew to a ~2-fold lower OD<sub>600</sub> compared to cultures at pH 6.0 or 7.0; however, following 20 h incubation, all three *P. aeruginosa* cultures reached comparable OD<sub>600</sub> values (Figure S6). The growth of *S. aureus* cultured at an initial pH of 5.0 was attenuated based on OD<sub>600</sub> values obtained at 8 and 20 h, which were ~1.5- to 2-fold lower at pH 5.0 compared to pH 6.0 and 7.0.

When cultured in the presence of CP-Ser at pH 7.0 or 6.0, comparable growth inhibition was observed for each bacterial pathogen (Figures 5 and S6), indicating that CP-Ser retains its antibacterial activity at pH 6.0. Further reduction of the initial culture pH to 5.0 attenuated the antimicrobial activity of CP-Ser against some bacterial species but not others. *E. coli* and *P. aeruginosa* remained susceptible to CP-Ser at pH 5.0, but negligible growth inhibition occurred for *S. Typhimurium*, *K. pneumoniae*, and *S. aureus* treated with up to 1000 µg/mL CP-Ser. *A. baumannii* growth was inhibited by CP-Ser at the 8 h timepoint, but growth recovery occurred by 20 h. We note that the ~2 mM Ca(II) ion concentration was employed in this assay because it is physiologically relevant; however, the analytical SEC studies (*vide supra*) suggest this concentration may be insufficient for complete tetramerization of CP, particularly at 1000 µg/mL, under mildly acidic conditions.

We also examined the activity of CP against five of these bacterial species and observed similar trends with the exception that growth of *K. pneumoniae* cultured at an initial pH of 5.0 was inhibited at the 8 h timepoint (Figures S7–S8). These observations indicate that the local pH is a factor that should be taken into account when considering the host-defense function of CP. In particular, the data suggest that (i) pH modulates the antibacterial activity of CP, (ii) some organisms are no longer susceptible to CP in acidic environments, and (iii) the effect of pH on the interplay between CP and bacterial pathogens must be considered on an organism-by-organism basis.

### **Mn(II) depletion from growth medium by CP is impaired at low pH.**

To provide initial insight into how low-pH regime may affect the metal-sequestering function of CP, we performed an unbiased assay that allows us to determine which metals CP depletes from microbial growth medium.<sup>11</sup> Although this assay does not provide quantitative information of metal binding affinities, it provides a helpful guide for further metal-binding studies and a simple format for evaluating various conditions. We treated MES:TSB medium adjusted to pH 5.0–7.0 with CP-Ser (250 µg/mL, 10.4 µM) in the absence and presence of a 2 mM Ca(II) supplement and used ICP-MS to quantify the metal levels remaining in the treated medium (filtrate) following removal of CP-Ser and its bound metals by spin filtration (Figures 6 and S9, Table S5). In agreement with prior work performed at pH 7.5,<sup>11</sup> ICP-MS analysis of treated medium samples at pH 7.0 revealed depletion of Mn, Fe, Cu, and Zn. Similar metal depletion profiles were obtained for samples buffered at pH 6.0. In contrast, when the MES:TSB medium was buffered at pH 5.0, the metal depletion profile markedly changed. In particular, the ability of CP-Ser to deplete Mn and Fe decreased in both the absence and presence of Ca(II), whereas Zn depletion was largely unaffected by low pH. This metal-depletion profile indicates that conditions at pH 5.0 favor Zn(II) sequestration over the multi-metal sequestration observed at pH 6.0–7.0. This observation is consistent with our previous studies that demonstrated a thermodynamic preference of the His<sub>6</sub> site according to Zn(II) > Fe(II) > Mn(II).<sup>10, 11</sup> Moreover, the His<sub>3</sub>Asp site of CP sequesters Zn(II), but not Mn(II) or Fe(II), and the combined contributions of both sites may facilitate Zn(II) sequestration at low pH. Lastly, to ascertain whether the depletion profile of CP-Ser at low pH vary between different growth media, we repeated this assay using MES:LB medium buffered to pH 5.0–7.0 (Figure S10 and Table

S6). Overall, we observed similar trends in both medium conditions in the absence and presence of Ca(II) ions.

Thus far, CP is the only known Mn(II)-sequestering host-defense protein, and its role in Mn(II) homeostasis at the host-pathogen interface has been demonstrated in various studies.<sup>6, 7, 9, 69–71</sup> The metal depletion data presented here provide initial insights into metal chelation by CP in low pH regimes, and reveal a lower capacity of CP to bind Mn(II) under these conditions, which motivated us to further study of the pH dependence of Mn(II) binding at the His<sub>6</sub> site.

### Analytical SEC supports reduced Mn(II) binding at low pH.

To provide an initial evaluation of Mn(II) binding by CP-Ser in the low-pH regime, we employed analytical SEC coupled with ICP-MS to examine samples containing the protein and excess Mn(II) ions. Our prior studies demonstrated that Mn(II) coordination to the His<sub>6</sub> site of CP-Ser in the absence of Ca(II) ions occurs with an apparent  $K_{d,Mn(II)}$  of ~5  $\mu$ M and promotes the self-association of heterodimers to form Mn(II)-bound heterotetramers.<sup>10, 20</sup> Guided by these studies, we incubated CP-Ser (200  $\mu$ M) with 10 equivalents of Mn(II) at pH 5.0–7.0 and analyzed the samples by SEC (Figure 7A and Table S7). In the pH 6.0–7.0 range, the presence of excess Mn(II) in the sample led to a peak shift to an elution volume (11.1 mL) between those of the apo CP-Ser heterodimer and Ca(II)-bound heterotetramer, as previously observed at pH 7.5.<sup>10</sup> At lower pH values, the elution volumes for samples containing excess Mn(II) were similar to those of apo CP-Ser. Quantification of the protein and Mn concentrations in the eluted fractions revealed that ~1 equivalent of Mn(II) was retained in the protein-containing fractions at pH 6.0, whereas a negligible amount of Mn(II) was found in the protein-containing fractions at pH 5.5 (Figures 7B–C and S11). When CP-Ser was incubated with both 10 equivalents of Mn(II) and 20 equivalents of Ca(II) at pH 5.5, a peak shift to a lower elution volume (11.3 mL) was observed and ~1 equivalent Mn(II) was retained during elution (Figure S11). Taken together, these data indicate that (i) at low pH and in the absence of Ca(II) ions, CP-Ser does not coordinate Mn(II) with sufficient affinity to retain the metal ion during elution, and (ii) Ca(II) binding at low pH increases the Mn(II) binding affinity, allowing CP to retain the metal during eluting. Overall, these observations are in agreement with the metal depletion assay results; both data sets indicate Ca(II)-dependent Mn(II) binding at low pH.

### Mn(II)-binding affinity of CP is pH-dependent.

To investigate how mildly acidic pH affects the Mn(II) binding affinity of CP-Ser, we performed Mn(II) competition titrations over the pH 5.5–7.0 range using the fluorescent metal-ion sensor Zinpyr-1 (ZP1). The apparent Mn(II) dissociation constant of ZP1 ( $K_{d,Mn(II)} = 550$  nM) was previously determined at pH 7.0.<sup>72</sup> In our early work at pH 7.5, we found that CP-Ser outcompeted ZP1 for 1 equivalent of Mn(II) when 20 equivalents of Ca(II) were present, providing an initial upper limit for the  $K_{d,Mn(II)}$  value of CP-Ser.<sup>10</sup> To extend these studies to low-pH regimes, we determined the apparent  $K_{d,Mn(II)}$  values of ZP1 at pH 6.0, and 5.5 by direct titrations monitored by fluorescence emission spectroscopy, which provided  $K_{d,Mn(II)}$  values of  $2.6 \pm 0.1$   $\mu$ M and  $9.6 \pm 0.5$   $\mu$ M at pH 6.0 and 5.5, respectively (Figure S12). When mixtures of ZP1 and CP-Ser were titrated with Mn(II) in

the absence of excess Ca(II) ions, ZP1 outcompeted the protein at each pH value, indicated by titration curves comparable to those of the ZP1 only controls (Figure 8). In contrast, when a mixture of ZP1, CP-Ser, and excess Ca(II) ions was titrated with Mn(II) at pH 7.0, negligible change in ZP1 emission occurred until ~1 equivalent of Mn(II) was added, and quenching of ZP1 emission followed (Figure 8). As expected, these data indicated that, in the presence of excess Ca(II) ions, CP-Ser outcompetes ZP1 for 1 equivalent of Mn(II) at pH 7.0. At pH 6.0, the titration curve for ZP1 and CP-Ser in the presence of excess Ca(II) ions revealed slight competition, suggesting a micromolar Mn(II) affinity for CP-Ser under these conditions. At pH 5.5, ZP1 outcompeted CP-Ser in the presence of Ca(II), indicating that the protein binds Mn(II) with  $K_{d, \text{Mn(II)}} > 9.6 \mu\text{M}$  under these conditions. Based on all available biochemical and spectroscopic studies reported to date, the His<sub>6</sub> site of CP coordinates Mn(II) with  $K_d < 10 \text{ nM}$  at pH 7.5 in the presence of Ca(II).<sup>9, 10, 12, 71</sup> Thus, these data indicate that a drop in pH from neutral to 5.5 results in at least a 1000-fold decrease in Mn(II) affinity such that CP is no longer able to sequester Mn(II).

### The His<sub>6</sub> Site Coordinates Mn(II) at low pH.

Next, we questioned whether the primary coordination sphere of the His<sub>6</sub> site that coordinates Mn(II) in a nearly idealized octahedral geometry at neutral pH changes under acidic conditions. In particular, we considered that the reduced Mn(II)-binding affinity at low pH could arise from protonation of one or more histidine residues at site 2, possibly resulting in a change in coordination number or a ligand substitution. To investigate these possibilities, we employed continuous-wave (CW) X-band EPR spectroscopy to probe the Mn(II)-His<sub>6</sub> site at low pH in the presence and absence of excess Ca(II) ions.<sup>10, 21</sup> We prepared samples of CP-Ser (200  $\mu\text{M}$ ) with 0.9 equivalents of Mn(II) and 20 equivalents of Ca(II) at pH 7.0, 6.0 and 5.5. In all cases, the EPR spectra were in agreement with our prior work<sup>10, 21</sup> and featured a well-defined sextet pattern with  $a = 8.8 \text{ mT}$  centered at  $g = 2.001$ , typical of the hyperfine-split  $M_s = \pm 1/2$  central-field transition of the <sup>55</sup>Mn(II) ion, and two formally forbidden  $m_s \pm 1$  and  $m_l \pm 1$  transitions within each sextet pair (Figure 9A). The positions of these transitions and the overall spectral line shapes and widths were unperturbed by low pH; however, a slight decrease in signal intensities occurred. We previously reported that point mutations in the His<sub>6</sub> site (e.g. His→Ala substitutions) resulted in reduced signal intensity and definition, and an increase in the intensities of the forbidden transitions relative to the allowed transitions.<sup>73</sup> Such features were not observed in the EPR spectra of Mn(II)-bound CP-Ser in the presence of Ca(II) at low pH. Overall, the prior and current spectroscopic data support a highly symmetric six-coordinate coordination environment for the Mn(II) center in the pH 5.0–7.5 range. Because this spectroscopy revealed no evidence for a change in the coordinating ligands, we speculate that formation of the Mn(II)-His<sub>6</sub> site at mildly acidic pH with reduced Mn(II)-binding affinity may indicate competitive protonation events of one or more His residues that compose this site.

We also prepared samples that did not include excess Ca(II) ions, and the spectrum obtained at pH 7.0 revealed a mixed population of Mn(II) bound to the His<sub>6</sub> site and unbound Mn(II) (Figure 9B), in agreement with our prior study performed at pH 7.5.<sup>10</sup> At lower pH (5.5–6.0), a significant decrease in the intensities of the EPR signals was observed, indicating that the samples predominantly contained unbound Mn(II). These results are in good agreement



with the analytical SEC/ICP-MS and Mn(II) competition titrations presented above, and demonstrate that Ca(II) ions are essential for Mn(II) binding in low-pH regimes.

### CP competes with bacterial Mn(II)-scavenging SBPs less effectively at low pH.

To acquire nutrient Mn(II) from the host, *S. aureus* and *Streptococcus pneumoniae* express the ATP-binding cassette Mn(II) transport systems MntABC and PsaABC, respectively.<sup>74, 75</sup> MntC and PsaA are solute binding proteins (SBP) that capture extracellular Mn(II). We recently evaluated the competition between CP and these SBPs and found that CP outcompeted both proteins for Mn(II) at pH 7.5 in the presence of excess Ca(II) ions.<sup>71</sup> To extend these analyses to low-pH regimes, we determined the Mn(II) speciation between the two SBPs and CP at pH 5.5–7.0 using a pull-down assay we previously reported using biotinylated CP (B-CP).<sup>71</sup> The Mn(II) speciation was evaluated under three different conditions: (i) addition of Mn(II) to a mixture of B-CP and MntC or PsaA, (ii) pre-incubating MntC or PsaA with Mn(II) followed by addition of B-CP, and (iii) pre-incubating B-CP with Mn(II) followed by addition of MntC or PsaA. After incubation (16 h, room temperature), B-CP was removed from the samples by pull-down with streptavidin resin (Figure S14), and the Mn(II) content of each solution was determined by ICP-MS analysis (Figures 10 and S13). In agreement with our prior observations, competitions performed at pH 7.0 revealed that <5% of Mn(II) remained in solution, indicating that B-CP outcompeted both SBPs for Mn(II) under these conditions. In contrast, for the competitions performed at pH 5.5–6.0, higher Mn(II) content (up to 30% of total added Mn(II)) was found in the solutions after B-CP removal. We employed analytical SEC combined with ICP-MS to probe the ability of MntC and PsaA to bind Mn(II) at low pH, and found that both SBPs eluted from the SEC column with ~1 equivalent of Mn(II) at pH 5.5 (Figure S15). Thus, the Mn(II) remaining in solution after pull-down of B-CP was presumably bound by the SBPs.

Preincubating either B-CP or the SBPs with Mn(II) had a negligible effect on the Mn(II) content of the solutions after pull down (Figure S13), suggesting that equilibrium was established during the timescale of the assay. Although CP coordinates Mn(II) with lower affinity at low pH, the pull-down assay results indicate that CP can compete with both SBPs for Mn(II) to a substantial degree even under mildly acidic conditions when excess Ca(II) ions are present. Nevertheless, the amount of Mn(II) bound to the SBPs, and transfer of these ions to MntAB and PsaBC for cellular uptake, may be sufficient to fulfill the nutritional Mn requirements of the pathogens expressing them in the presence of CP.

## Discussion

This work provides an initial report of how changes in pH influence the biochemical and functional properties of CP, including Ca(II) binding and self-association, transition metal complexation, and antimicrobial activity. These observations provide new perspectives on the working model for CP and a foundation for future studies broadly aimed at conceptualizing how chemically diverse host environments affect the function of this remarkable host-defense protein.

The interplay between Ca(II) ions and CP is central to our current picture of how CP functions in the extracellular space. At neutral and slightly alkaline pH, Ca(II) binding to CP

heterodimers promotes the self-assembly of heterotetramers, enhances protease stability, and increases the transition metal binding affinities such that CP can sequester multiple divalent transition metal ions.<sup>12</sup> Our current studies reveal that at least 5-fold higher Ca(II) equivalents are required for CP to fully heterotetramerize at pH 5.5 compared to neutral pH, and that mildly acidic pH also shifts the heterotetramer-heterodimer equilibrium towards the heterodimer. Based on prior studies of quaternary structure, the Ca(II)-bound heterotetramer is expected to be the abundant extracellular form unless the protein scaffold undergoes methionine oxidation, which results in mixtures of heterodimers and heterotetramers.<sup>8, 12, 65</sup> The current results indicate a more nuanced picture where pH also impacts the speciation of CP oligomers in the extracellular space. CP may exist as a mixture of apo heterodimers, Ca(II)-bound heterodimers and Ca(II)-bound heterotetramers in mildly acidic microenvironments. Since CP heterodimers are more susceptible to proteolytic degradation than the Ca(II)-bound heterotetramers,<sup>20</sup> the current results also suggest that accelerated degradation of CP by host and bacterial proteases active at low pH can occur in acidic locales, a scenario that warrants further investigation.

The transition metal binding properties of CP are complex and, in this work, we focused on evaluating how changes in pH affect Mn(II) chelation. Our studies indicate that Ca(II) binding enhances the Mn(II) affinity of CP and promote the formation of the Mn(II)-His<sub>6</sub> site across the pH 5.5–7.0 range. Nevertheless, the Mn(II)-binding affinity of the His<sub>6</sub> site is drastically reduced at pH 5.5; consequently, CP withholds Mn(II) less effectively from two bacterial SBPs at this pH. Taken together, these results indicate that even in the presence of excess Ca(II) ions, mildly acidic pH compromises the ability of CP to sequester Mn(II). This conclusion can be considered in the context of prior work focused on the competition between CP and pathogens for Mn(II). These prior studies demonstrated that CP reduces cell-associated Mn levels in diverse microbial pathogens at near-neutral pH.<sup>19, 67, 68, 76, 77</sup> Moreover, seminal studies of the interplay between CP and *S. aureus* revealed that CP induces a Mn starvation response in *S. aureus* characterized by expression of the Mn(II) acquisition machinery of *mntABC* and *mntH*.<sup>6, 70</sup> Similar behavior was later reported for *S. Typhimurium*.<sup>78</sup> Nevertheless, several investigations employing murine models of infection indicated that *S. aureus* and *S. Typhimurium* can evade Mn(II) starvation caused by CP.<sup>70, 78</sup> Broadly, these studies revealed the importance of bacterial adaptation as a strategy that enables pathogens to overcome the metal-withholding innate immune response. Our results indicate that CP no longer functions as a Mn(II) sequestering protein at mildly acidic pH, which would be advantageous for microbial pathogens that require on this nutrient when colonizing the host, and provide another perspective on host-microbe interactions that occur in environments where the pH may be reduced compared to normal homeostatic conditions.

Looking beyond Mn(II), this study provides a foundation for further investigations on several fronts. Acidic conditions are expected to impact the binding affinity of CP for all divalent first-row transition metal ions, necessitating additional chemical and biological studies that delineate whether the protein retains the capacity to sequester Fe(II) and Zn(II) at low pH. Although the metal depletion profile of CP at low pH indicated that Fe depletion is attenuated under these conditions, these experiments were performed aerobically and in the absence of an exogenous reducing agent, which will favor the Fe(III) oxidation state of iron. Because the Fe redox speciation and the effect of a reducing environment on metal

depletion were not addressed in this study,<sup>79</sup> the results may underestimate the capacity of CP to coordinate Fe(II) under weakly acidic conditions. Thus, further investigations of Fe(II) chelation by CP in mildly acidic pH regimes is necessary. Likewise, additional studies of Zn(II) binding are warranted. In contrast to the results for Mn and Fe, low pH had negligible effect on the Zn depletion profile of CP, which raises the possibility that CP may selectively sequester Zn(II) at low pH. We reason that the effect of acidic conditions on Zn(II) sequestration may be less profound because binding of this metal ion is thermodynamically preferred, both the His<sub>3</sub>Asp and His<sub>6</sub> sites participate in this function, and both the heterodimer and heterotetramer bind Zn(II) with high affinity.<sup>8, 17</sup>

The broad-spectrum antimicrobial activity of CP is attributed to its ability to sequester multiple transition metal ions, which limits the growth of microbial pathogens with different metal requirements.<sup>12</sup> The initial assessment of how culture pH affects the antimicrobial activity of CP against six bacterial pathogens presented here revealed different microbial responses to CP under mildly acidic pH, highlighting the need to approach this issue on a case-by-case basis. Interpreting such studies requires that we advance our understanding about the cross-talk between environmental pH and metalloregulatory processes as well as metal homeostasis in microbial pathogens. Making headway along these lines will also reveal fundamental aspects of microbial physiology as well as mechanisms of microbial pathogenesis.

## Conclusions

In closing, CP is deployed to sequester nutrient metal ions in chemically complex and diverse environments. This work provides a first effort at incorporating pH into the working model for the extracellular metal-sequestering function of CP. The current results complement prior studies that suggest the chemical complexity of infection sites modulates the metal-withholding activity of CP.<sup>65, 66, 78</sup> Together, these efforts begin to provide a picture where components of multi-metal sequestration by CP may be enabled or disabled depending on the chemical composition of a given biological site. We look forward to learning the outcomes of future efforts that further address this possibility.

## Supplementary Material

Refer to Web version on PubMed Central for supplementary material.

## Acknowledgements

This work was supported by the NIH (R01 GM126376). The ICP-MS instrument at MIT is maintained by the MIT Center for Environmental Health Sciences (NIH P30-ES002109). CD spectroscopy instrumentation is provided by the MIT Biophysical Instrumentation Facility for the Study of Complex Macromolecular Systems is supported by NSF grant 0070319. EPR instrumentation is housed in the Department of Chemistry Instrumentation Facility. The *S. aureus* USA300 JE2 strain was obtained from the Network on Antimicrobial Resistance in Staphylococcus aureus (NARSA) program supported under National Institute of Allergy and Infectious Diseases Contract HHSN272200700055C.

## Abbreviations

AMA                      antimicrobial activity

<b>ASL</b>	airway surface liquid
<b>ATCC</b>	American Type Culture Collection
<b>ATR</b>	acid tolerance response
<b>CD</b>	circular dichroism
<b>CF</b>	cystic fibrosis
<b>CP</b>	calprotectin (including CP-Ser, the Cys→Ser variant)
<b>B-CP</b>	biotinylated calprotectin
<b>mCP</b>	murine calprotectin
<b>EPR</b>	electron paramagnetic resonance
<b>IBD</b>	inflammatory bowel disease
<b>ICP-MS</b>	inductively-coupled plasma mass spectrometry
<b>LB</b>	lysogeny broth
<b>LF</b>	lactoferrin
<b>MES 2</b>	-( <i>N</i> -morpholino)ethanesulfonic acid
<b>SBP</b>	solute-binding protein
<b>SEC</b>	size-exclusion chromatography
<b>SEM</b>	standard error of the mean
<b>TF</b>	transferrin
<b><math>T_m</math></b>	melting temperature
<b>TSB</b>	tryptic soy broth
<b>ZPI</b>	Zinpyr-1

## References

- [1]. Hood MI, and Skaar EP (2012) Nutritional immunity: transition metals at the pathogen-host interface, *Nat. Rev. Microbiol* 10, 525–537. [PubMed: 22796883]
- [2]. Weinberg ED (1975) Nutritional immunity: host's attempt to withhold iron from microbial invaders, *JAMA* 231, 39–41. [PubMed: 1243565]
- [3]. Johne B, Fagerhol MK, Lyberg T, Prydz H, Brandtzaeg P, Naess-Andresen CF, and Dale I (1997) Functional and clinical aspects of the myelomonocyte protein calprotectin, *Mol. Pathol* 50, 113–123. [PubMed: 9292145]
- [4]. Edgeworth J, Gorman M, Bennett R, Freemont P, and Hogg N (1991) Identification of p8,14 as a highly abundant heterodimeric calcium binding protein complex of myeloid cells, *J. Biol. Chem* 266, 7706–7713. [PubMed: 2019594]

- [5]. Steinbakk M, Naess-Andresen CF, Lingaas E, Dale I, Brandtzaeg P, and Fagerhol MK (1990) Antimicrobial actions of calcium binding leucocyte L1 protein, calprotectin, *The Lancet* 336, 763–765.
- [6]. Corbin BD, Seeley EH, Raab A, Feldmann J, Miller MR, Torres VJ, Anderson KL, Dattilo BM, Dunman PM, Gerads R, Caprioli RM, Nacken W, Chazin WJ, and Skaar EP (2008) Metal chelation and inhibition of bacterial growth in tissue abscesses, *Science* 319, 962–965. [PubMed: 18276893]
- [7]. Kehl-Fie TE, Chitayat S, Hood MI, Damo S, Restrepo N, Garcia C, Munro KA, Chazin WJ, and Skaar EP (2011) Nutrient metal sequestration by calprotectin inhibits bacterial superoxide defense, enhancing neutrophil killing of *Staphylococcus aureus*, *Cell Host Microbe* 10, 158–164. [PubMed: 21843872]
- [8]. Brophy MB, Hayden JA, and Nolan EM (2012) Calcium ion gradients modulate the zinc affinity and antibacterial activity of human calprotectin, *J. Am. Chem. Soc* 134, 18089–18100. [PubMed: 23082970]
- [9]. Damo SM, Kehl-Fie TE, Sugitani N, Holt ME, Rathi S, Murphy WJ, Zhang Y, Betz C, Hench L, Fritz G, Skaar EP, and Chazin WJ (2013) Molecular basis for manganese sequestration by calprotectin and roles in the innate immune response to invading bacterial pathogens, *Proc. Natl. Acad. Sci. U.S.A* 110, 3841–3846. [PubMed: 23431180]
- [10]. Hayden JA, Brophy MB, Cunden LS, and Nolan EM (2013) High-affinity manganese coordination by human calprotectin is calcium-dependent and requires the histidine-rich site formed at the dimer interface, *J. Am. Chem. Soc* 135, 775–787. [PubMed: 23276281]
- [11]. Nakashige TG, Zhang B, Krebs C, and Nolan EM (2015) Human calprotectin is an iron-sequestering host-defense protein, *Nat. Chem. Biol* 11, 765–771. [PubMed: 26302479]
- [12]. Zygiel EM, and Nolan EM (2018) Transition metal sequestration by the host-defense protein calprotectin, *Annu. Rev. Biochem* 87, 621–643. [PubMed: 29925260]
- [13]. Hunter MJ, and Chazin WJ (1998) High level expression and dimer characterization of the S100 EF-hand proteins, migration inhibitory factor-related proteins 8 and 14, *J. Biol. Chem* 273, 12427–12435. [PubMed: 9575199]
- [14]. Leukert N, Vogl T, Strupat K, Reichelt R, Sorg C, and Roth J (2006) Calcium-dependent tetramer formation of S100A8 and S100A9 is essential for biological activity, *J. Mol. Biol* 359, 961–972. [PubMed: 16690079]
- [15]. Korndörfer IP, Brueckner F, and Skerra A (2007) The crystal structure of the human (S100A8/S100A9)<sub>2</sub> heterotetramer, calprotectin, illustrates how conformational changes of interacting  $\alpha$ -helices can determine specific association of two EF-hand proteins, *J. Mol. Biol* 370, 887–898. [PubMed: 17553524]
- [16]. Strupat K, Rogniaux H, Van Dorsselaer A, Roth J, and Vogl T (2000) Calcium-induced noncovalently linked tetramers of MRP8 and MRP14 are confirmed by electrospray ionization-mass analysis, *J. Am. Soc. Mass. Spectrom* 11, 780–788. [PubMed: 10976885]
- [17]. Nakashige TG, Stephan JR, Cunden LS, Brophy MB, Wommack AJ, Keegan BC, Shearer JM, and Nolan EM (2016) The hexahistidine motif of host-defense protein human calprotectin contributes to zinc withholding and its functional versatility, *J. Am. Chem. Soc* 138, 12243–12251. [PubMed: 27541598]
- [18]. Nakashige TG, Zygiel EM, Drennan CL, and Nolan EM (2017) Nickel sequestration by the host-defense protein human calprotectin, *J. Am. Chem. Soc* 139, 8828–8836. [PubMed: 28573847]
- [19]. Besold AN, Gilston BA, Radin JN, Ramsoomair C, Culbertson EM, Li CX, Cormack BP, Chazin WJ, Kehl-Fie TE, and Culotta VC (2018) Role of calprotectin in withholding zinc and copper from *Candida albicans*, *Infect. Immun* 86, e00779–17. [PubMed: 29133349]
- [20]. Stephan JR, and Nolan EM (2016) Calcium-induced tetramerization and zinc chelation shield human calprotectin from degradation by host and bacterial extracellular proteases, *Chem. Sci* 7, 1962–1975. [PubMed: 26925211]
- [21]. Gagnon DM, Brophy MB, Bowman SEJ, Stich TA, Drennan CL, Britt RD, and Nolan EM (2015) Manganese binding properties of human calprotectin under conditions of high and low calcium: X-ray crystallographic and advanced electron paramagnetic resonance spectroscopic analysis, *J. Am. Chem. Soc* 137, 3004–3016. [PubMed: 25597447]

- [22]. Nugent SG, Kumar D, Rampton DS, and Evans DF (2001) Intestinal luminal pH in inflammatory bowel disease: possible determinants and implications for therapy with aminosalicylates and other drugs, *Gut* 48, 571–577. [PubMed: 11247905]
- [23]. Ravel J, Gajer P, Abdo Z, Schneider GM, Koenig SSK, McCulle SL, Karlebach S, Gorle R, Russell J, Tacket CO, Brotman RM, Davis CC, Ault K, Peralta L, and Forney LJ (2011) Vaginal microbiome of reproductive-age women, *Proc. Natl. Acad. Sci. U.S.A* 108, 4680–4687. [PubMed: 20534435]
- [24]. Elias PM (2007) The skin barrier as an innate immune element, *Semin. Immunopathol* 29, 3–14. [PubMed: 17621950]
- [25]. Huynh KK, and Grinstein S (2007) Regulation of vacuolar pH and its modulation by some microbial species, *Microbiol. Mol. Biol. Rev* 71, 452–462. [PubMed: 17804666]
- [26]. Tate S, MacGregor G, Davis M, Innes JA, and Greening AP (2002) Airways in cystic fibrosis are acidified: detection by exhaled breath condensate, *Thorax* 57, 926–929. [PubMed: 12403872]
- [27]. Lund P, Tramonti A, and De Biase D (2014) Coping with low pH: molecular strategies in neutrophilic bacteria, *FEMS Microbiol. Rev* 38, 1091–1125. [PubMed: 24898062]
- [28]. De Angelis M, and Gobbetti M (2004) Environmental stress responses in *Lactobacillus*: A review, *Proteomics* 4, 106–122. [PubMed: 14730676]
- [29]. Broadbent JR, Larsen RL, Deibel V, and Steele JL (2010) Physiological and transcriptional response of *Lactobacillus casei* ATCC 334 to acid stress, *J. Bacteriol* 192, 2445–2458. [PubMed: 20207759]
- [30]. Kanjee U, and Houry WA (2013) Mechanisms of acid resistance in *Escherichia coli*, *Annu. Rev. Microbiol* 67, 65–81. [PubMed: 23701194]
- [31]. Álvarez-Ordóñez A, Begley M, Prieto M, Messens W, López M, Bernardo A, and Hill C (2011) *Salmonella* spp. survival strategies within the host gastrointestinal tract, *Microbiology* 157, 3268–3281. [PubMed: 22016569]
- [32]. Ryan D, Pati NB, Ojha UK, Padhi C, Ray S, Jaiswal S, Singh GP, Mannala GK, Schultze T, Chakraborty T, and Suar M (2015) Global transcriptome and mutagenic analyses of the acid tolerance response of *Salmonella enterica* serovar Typhimurium, *Appl. Environ. Microbiol* 81, 8054–8065. [PubMed: 26386064]
- [33]. Sachs G, Weeks DL, Melchers K, and Scott DR (2003) The gastric biology of *Helicobacter pylori*, *Annu. Rev. Physiol* 65, 349–369. [PubMed: 12471160]
- [34]. Jones MD, Li Y, and Zamble DB (2018) Acid-responsive activity of the *Helicobacter pylori* metalloregulator NikR, *Proc. Natl. Acad. Sci. U.S.A* 115, 8966–8971. [PubMed: 30126985]
- [35]. Maroncle N, Rich C, and Forestier C (2006) The role of *Klebsiella pneumoniae urease* in intestinal colonization and resistance to gastrointestinal stress, *Res. Microbiol* 157, 184–193. [PubMed: 16139482]
- [36]. Cotter PD, and Hill C (2003) Surviving the acid test: responses of gram-positive bacteria to low pH, *Microbiol. Mol. Biol. Rev* 67, 429–453. [PubMed: 12966143]
- [37]. Bore E, Langsrud S, Langsrud Ø, Rode TM, and Holck A (2007) Acid-shock responses in *Staphylococcus aureus* investigated by global gene expression analysis, *Microbiology* 153, 2289–2303. [PubMed: 17600073]
- [38]. Smith JL, Liu Y, and Paoli GC (2012) How does *Listeria monocytogenes* combat acid conditions?, *Can. J. Microbiol* 59, 141–152. [PubMed: 23540331]
- [39]. Vylkova S, Carman AJ, Danhof HA, Collette JR, Zhou H, and Lorenz MC (2011) The fungal pathogen *Candida albicans* autoinduces hyphal morphogenesis by raising extracellular pH, *mBio* 2, e00055–11. [PubMed: 21586647]
- [40]. Papp-Wallace KM, and Maguire ME (2006) Manganese transport and the role of manganese in virulence, *Annu. Rev. Microbiol* 60, 187–209. [PubMed: 16704341]
- [41]. Lau CKY, Krewulak KD, and Vogel HJ (2015) Bacterial ferrous iron transport: the Feo system, *FEMS Microbiol. Rev* 40, 273–298. [PubMed: 26684538]
- [42]. Wyckoff EE, Mey AR, Leimbach A, Fisher CF, and Payne SM (2006) Characterization of ferric and ferrous iron transport systems in *Vibrio cholerae*, *J. Bacteriol* 188, 6515–6523. [PubMed: 16952942]

- [43]. Gancz H, Censini S, and Merrell DS (2006) Iron and pH homeostasis intersect at the level of Fur regulation in the gastric pathogen *Helicobacter pylori*, *Infect. Immun* 74, 602–614. [PubMed: 16369017]
- [44]. Choi E, Groisman EA, and Shin D (2009) Activated by different signals, the PhoP/PhoQ two-component system differentially regulates metal uptake, *J. Bacteriol* 191, 7174–7181. [PubMed: 19801407]
- [45]. Brickman TJ, and Armstrong SK (2012) Iron and pH-responsive FtrABCD ferrous iron utilization system of *Bordetella* species, *Mol. Microbiol* 86, 580–593. [PubMed: 22924881]
- [46]. Colomer-Winter C, Flores-Mireles AL, Baker SP, Frank KL, Lynch AJL, Hultgren SJ, Kitten T, and Lemos JA (2018) Manganese acquisition is essential for virulence of *Enterococcus faecalis*, *PLOS Pathog* 14, e1007102. [PubMed: 30235334]
- [47]. Lee IH, Cho Y, and Lehrer RI (1997) Effects of pH and salinity on the antimicrobial properties of clavanins, *Infect. Immun* 65, 2898–2903. [PubMed: 9199465]
- [48]. Abou Alaiwa MH, Reznikov LR, Gansemer ND, Sheets KA, Horswill AR, Stoltz DA, Zabner J, and Welsh MJ (2014) pH modulates the activity and synergism of the airway surface liquid antimicrobials  $\beta$ -defensin-3 and LL-37, *Proc. Natl. Acad. Sci. U.S.A* 111, 18703–18708. [PubMed: 25512526]
- [49]. Malik E, Dennison SR, Harris F, and Phoenix DA (2016) pH dependent antimicrobial peptides and proteins, their mechanisms of action and potential as therapeutic agents, *Pharmaceuticals* 9, 67.
- [50]. Cole AM, Kim Y-H, Tahk S, Hong T, Weis P, Waring AJ, and Ganz T (2001) Calcitermin, a novel antimicrobial peptide isolated from human airway secretions, *FEBS Lett* 504, 5–10. [PubMed: 11522286]
- [51]. Cole AM, Dewan P, and Ganz T (1999) Innate antimicrobial activity of nasal secretions, *Infect. Immun* 67, 3267–3275. [PubMed: 10377100]
- [52]. Pezzulo AA, Tang XX, Hoegger MJ, Abou Alaiwa MH, Ramachandran S, Moninger TO, Karp PH, Wohlford-Lenane CL, Haagsman HP, van Eijk M, Bánfi B, Horswill AR, Stoltz DA, McCray PB, Welsh MJ, and Zabner J (2012) Reduced airway surface pH impairs bacterial killing in the porcine cystic fibrosis lung, *Nature* 487, 109–113. [PubMed: 22763554]
- [53]. Sun H, Li H, and Sadler PJ (1999) Transferrin as a metal ion mediator, *Chem. Rev* 99, 2817–2842. [PubMed: 11749502]
- [54]. Luck AN, and Mason AB (2012) Chapter one - transferrin-mediated cellular iron delivery, *Curr. Top. Membr* 69, 3–35. [PubMed: 23046645]
- [55]. Friedman DB, Stauff DL, Pishchany G, Whitwell CW, Torres VJ, and Skaar EP (2006) *Staphylococcus aureus* redirects central metabolism to increase iron availability, *PLOS Pathog* 2, e87. [PubMed: 16933993]
- [56]. Baker HM, and Baker EN (2012) A structural perspective on lactoferrin function, *Biochem. Cell Biol* 90, 320–328. [PubMed: 22292559]
- [57]. Dorin JR, Novak M, Hill RE, Brock DJH, Secher DS, and van Heyningen V (1987) A clue to the basic defect in cystic fibrosis from cloning the CF antigen gene, *Nature* 326, 614–617. [PubMed: 3561500]
- [58]. Aadland E, and Fagerhol MK (2002) Faecal calprotectin: a marker of inflammation throughout the intestinal tract, *Eur. J. Gastroenterol. Hepatol* 14, 823–825. [PubMed: 12172400]
- [59]. Edgcomb SP, and Murphy KP (2002) Variability in the pKa of histidine side-chains correlates with burial within proteins, *Proteins* 49, 1–6. [PubMed: 12211010]
- [60]. Grimsley GR, Scholtz JM, and Pace CN (2009) A summary of the measured pK values of the ionizable groups in folded proteins, *Protein Sci* 18, 247–251. [PubMed: 19177368]
- [61]. Wang Q, Aleshintsev A, Jose AN, Aramini JM, and Gupta R Calcium regulates S100A12 zinc sequestration by limiting structural variations, *ChemBioChem* 21, 1372–1382.
- [62]. Vogl T, Leukert N, Barczyk K, Strupat K, and Roth J (2006) Biophysical characterization of S100A8 and S100A9 in the absence and presence of bivalent cations, *Biochim. Biophys. Acta* 1763, 1298–1306. [PubMed: 17050004]

- [63]. Hadley RC, Gu Y, and Nolan EM (2018) Initial biochemical and functional evaluation of murine calprotectin reveals Ca(II)-dependence and its ability to chelate multiple nutrient transition metal ions, *Biochemistry* 57, 2846–2856. [PubMed: 29659256]
- [64]. Nakashige TG, Bowman SEJ, Zygiel EM, Drennan CL, and Nolan EM (2018) Biophysical examination of the calcium-modulated nickel-binding properties of human calprotectin reveals conformational change in the EF-hand domains and His<sub>3</sub>Asp site, *Biochemistry* 57, 4155–4164. [PubMed: 29890074]
- [65]. Stephan JR, Yu F, Costello RM, Bleier BS, and Nolan EM (2018) Oxidative post-translational modifications accelerate proteolytic degradation of calprotectin, *J. Am. Chem. Soc* 140, 17444–17455. [PubMed: 30380834]
- [66]. Liu JZ, Jellbauer S, Poe AJ, Ton V, Pesciaroli M, Kehl-Fie TE, Restrepo NA, Hosking MP, Edwards RA, Battistoni A, Pasquali P, Lane TE, Chazin WJ, Vogl T, Roth J, Skaar EP, and Raffatellu M (2012) Zinc sequestration by the neutrophil protein calprotectin enhances *Salmonella* growth in the inflamed gut, *Cell Host Microbe* 11, 227–239. [PubMed: 22423963]
- [67]. Wang J, Lonergan ZR, Gonzalez-Gutierrez G, Nairn BL, Maxwell CN, Zhang Y, Andreini C, Karty JA, Chazin WJ, Trinidad JC, Skaar EP, and Giedroc DP (2019) Multi-metal restriction by calprotectin impacts de novo flavin biosynthesis in *Acinetobacter baumannii*, *Cell Chem. Biol* 26, 745–755. [PubMed: 30905682]
- [68]. Zygiel EM, Nelson CE, Brewer LK, Oglesby-Sherrouse AG, and Nolan EM (2019) The human innate immune protein calprotectin induces iron starvation responses in *Pseudomonas aeruginosa*, *J. Biol. Chem* 294, 3549–3562. [PubMed: 30622135]
- [69]. Brophy MB, and Nolan EM (2015) Manganese and microbial pathogenesis: sequestration by the mammalian immune system and utilization by microorganisms, *ACS Chem. Biol* 10, 641–651. [PubMed: 25594606]
- [70]. Kehl-Fie TE, Zhang Y, Moore JL, Farrand AJ, Hood MI, Rathi S, Chazin WJ, Caprioli RM, and Skaar EP (2013) MntABC and MntH contribute to systemic *Staphylococcus aureus* infection by competing with calprotectin for nutrient manganese, *Infect. Immun* 81, 3395–3405. [PubMed: 23817615]
- [71]. Hadley RC, Gagnon DM, Brophy MB, Gu Y, Nakashige TG, Britt RD, and Nolan EM (2018) Biochemical and spectroscopic observation of Mn(II) sequestration from bacterial Mn(II) transport machinery by calprotectin, *J. Am. Chem. Soc* 140, 110–113. [PubMed: 29211955]
- [72]. You Y, Tomat E, Hwang K, Atanasijevic T, Nam W, Jasanoff AP, and Lippard SJ (2010) Manganese displacement from Zinpyr-1 allows zinc detection by fluorescence microscopy and magnetic resonance imaging, *Chem. Commun* 46, 4139–4141.
- [73]. Brophy MB, Nakashige TG, Gaillard A, and Nolan EM (2013) Contributions of the S100A9 C-terminal tail to high-affinity Mn(II) chelation by the host-defense protein human calprotectin, *J. Am. Chem. Soc* 135, 17804–17817. [PubMed: 24245608]
- [74]. Eijkelkamp BA, McDevitt CA, and Kitten T (2015) Manganese uptake and streptococcal virulence, *BioMetals* 28, 491–508. [PubMed: 25652937]
- [75]. Gribenko AV, Liberator P, Anderson AS, Matsuka YV, and Mosyak L (2015) Cell surface antigen - manganese-binding protein MntC from *Staphylococcus aureus*, In *Encyclopedia of Inorganic and Bioinorganic Chemistry* (Scott RA, Ed.), John Wiley & Sons, Ltd.
- [76]. Besold AN, Culbertson EM, Nam L, Hobbs RP, Boyko A, Maxwell CN, Chazin WJ, Marques AR, and Culotta VC (2018) Antimicrobial action of calprotectin that does not involve metal withholding, *Metallomics* 10, 1728–1742. [PubMed: 30206620]
- [77]. Radin JN, Zhu J, Brazel EB, McDevitt CA, and Kehl-Fie TE (2019) Synergy between nutritional immunity and independent host defenses contributes to the importance of the MntABC manganese transporter during *Staphylococcus aureus* infection, *Infect. Immun* 87, e00642–18. [PubMed: 30348827]
- [78]. Diaz-Ochoa VE, Lam D, Lee CS, Klaus S, Behnsen J, Liu JZ, Chim N, Nuccio S-P, Rathi SG, Mastroianni JR, Edwards RA, Jacobo CM, Cerasi M, Battistoni A, Ouellette AJ, Goulding CW, Chazin WJ, Skaar EP, and Raffatellu M (2016) *Salmonella* mitigates oxidative stress and thrives in the inflamed gut by evading calprotectin-mediated manganese sequestration, *Cell Host Microbe* 19, 814–825. [PubMed: 27281571]



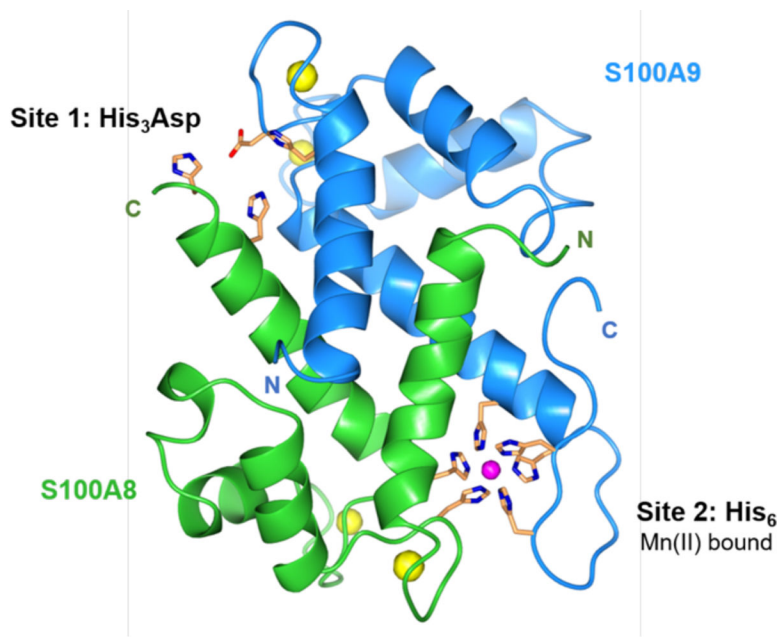
- [79]. Nakashige TG, and Nolan EM (2017) Human calprotectin affects the redox speciation of iron, *Metallomics* 9, 1086–1095. [PubMed: 28561859]

Author Manuscript

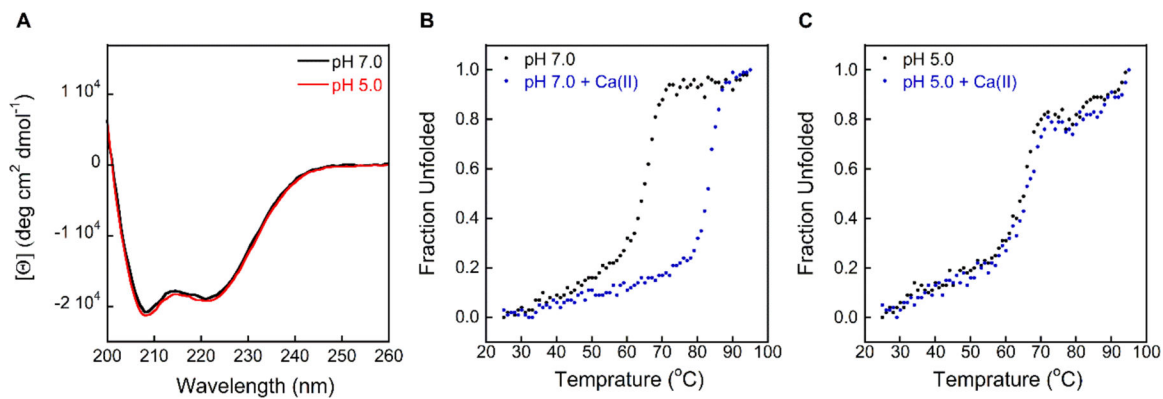
Author Manuscript

Author Manuscript

Author Manuscript

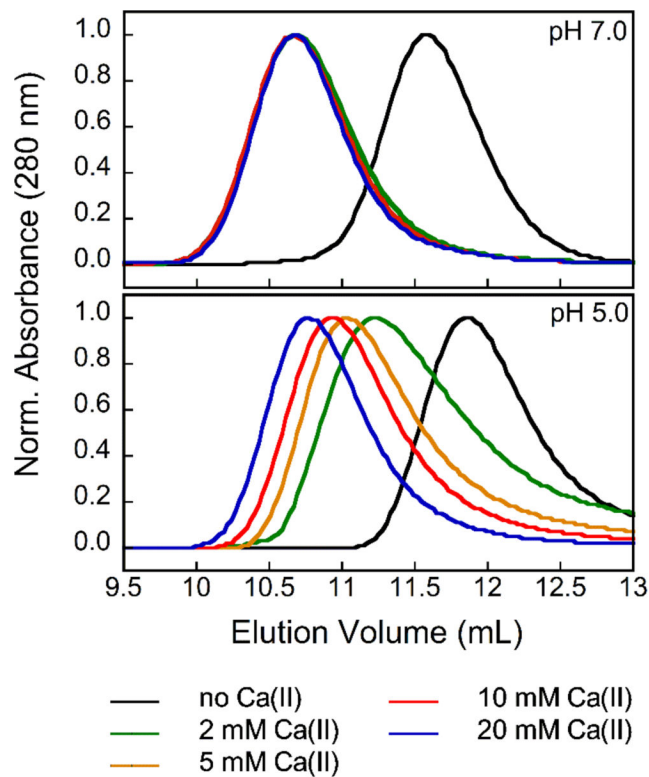


**Figure 1.** Crystal structure of Mn(II)-, Ca(II)-, and Na(I)-bound CP-Ser (PDB 4XJK).<sup>21</sup> A heterodimer unit of S100A8 (green) and S100A9 (blue) is taken from the structure of the heterotetramer. The N- and C-termini of S100A8 and S100A9 are labeled. Mn(II) is shown in magenta; Ca(II) and Na(I) are shown in yellow. The transition-metal binding residues are shown in orange.



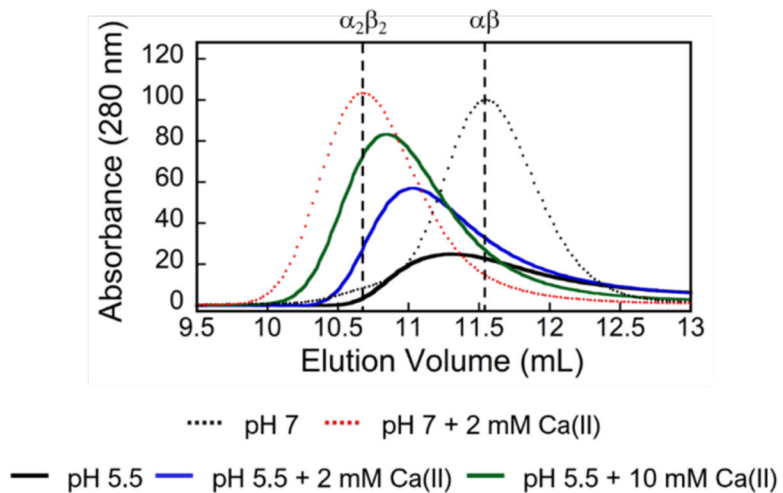
**Figure 2.**

CD spectra and thermal denaturation of CP-Ser at pH 5.0 and 7.0 (10 mM MES buffer). (A) CP-Ser exhibits similar CD features at pH 7.0 (black) and 5.0 (red). (B-C) Thermal denaturation of CP-Ser at pH 7.0 and 5.0 in the absence (black) and presence (blue) of 2 mM Ca(II). The CD spectra of CP and CP-Ser in the presence and absence of Ca(II) at pH 5.0–7.0 are presented in Figures S1–S2. Thermal denaturation plots of CP-Ser at pH 5.5–6.0 are presented in Figure S3.



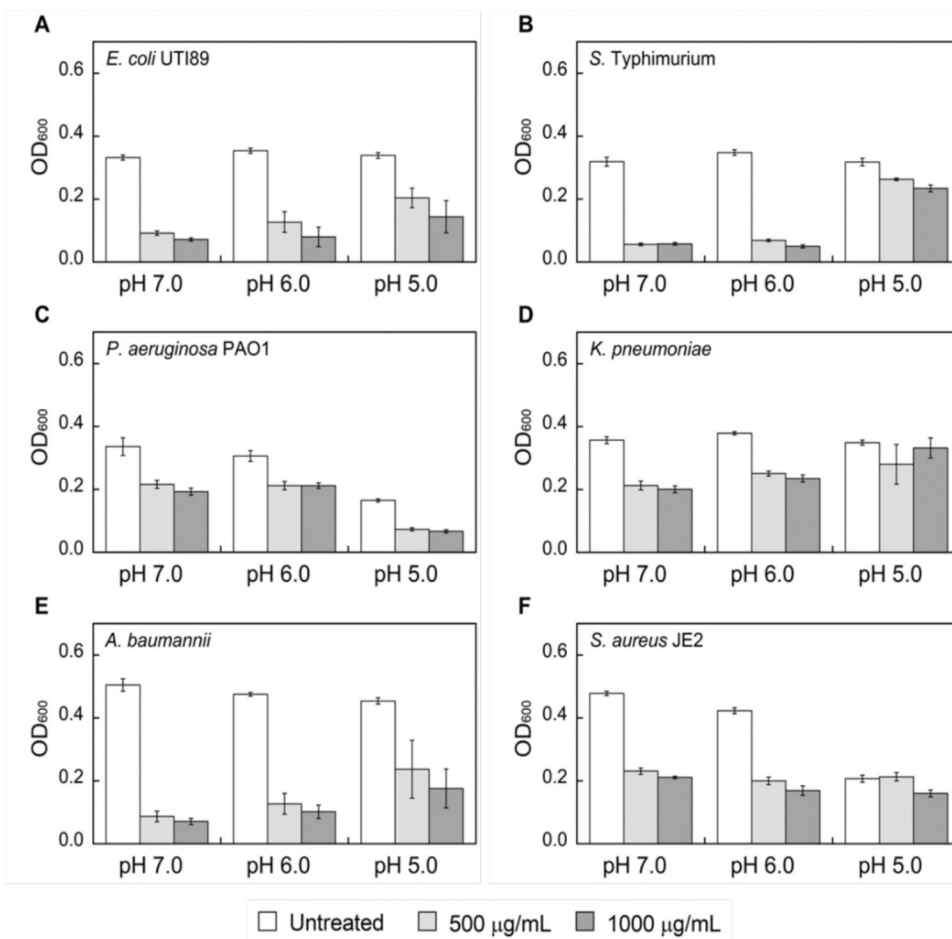
**Figure 3.**

Analytical SEC chromatograms of CP-Ser (100  $\mu$ M) in the absence and presence of 2, 5, 10 and 20 mM Ca(II) (75 mM MES, 100 mM NaCl, pH 5.0 or 7.0) at 4  $^{\circ}$ C. Each chromatogram was normalized to a maximum absorbance of 1. Chromatograms at pH 5.5–6.5 are provided in Figure S5. Elution volumes and corresponding molecular weights are given in Table S4.

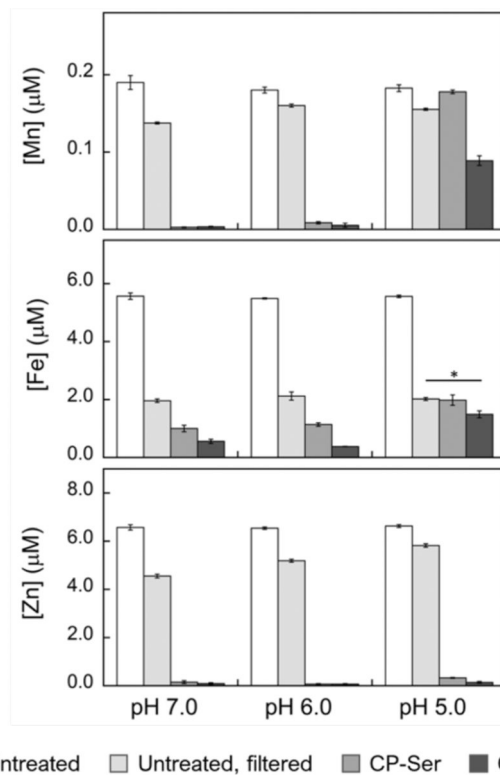


**Figure 4.**

Analytical SEC chromatograms of CP-Ser (100 μM) in the absence (black dashed line,  $\alpha\beta$ ) and presence (red dashed line,  $\alpha_2\beta_2$ ) of 2 mM Ca(II) at pH 7.0 (75 mM MES, 100 mM NaCl). Following incubation in the presence of 2 mM Ca(II) at pH 7.0, the pH was adjusted to 5.5 and the sample was eluted with MES buffer (75 mM MES, 100 mM NaCl, pH 5.5) without Ca(II) supplementation (black line) or with either 2 mM Ca(II) (blue line) or 10 mM Ca(II) (green line).

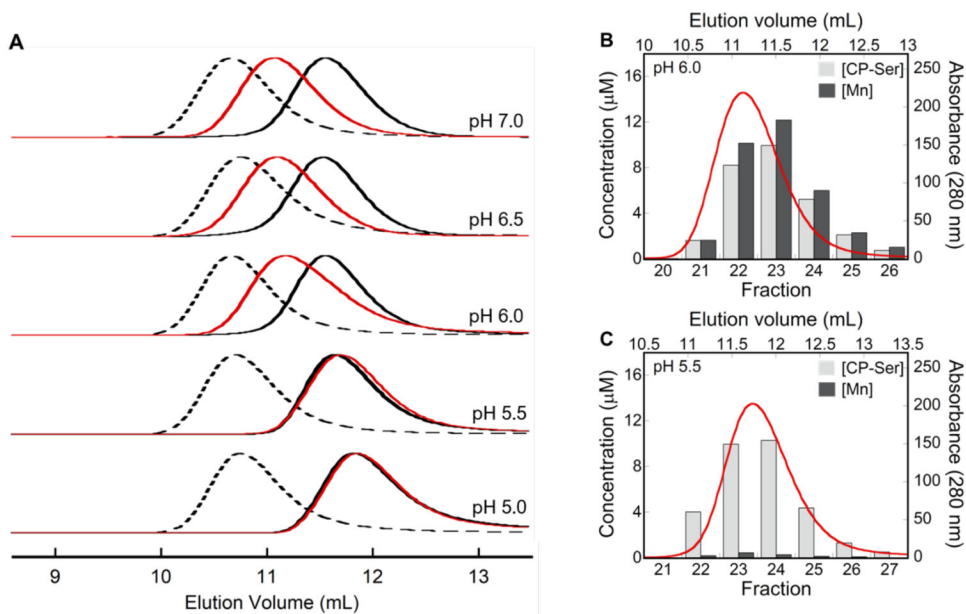


**Figure 5.** Growth inhibitory activity of CP-Ser against *E. coli* UTI89 (A), *S. Typhimurium* (B), *P. aeruginosa* PAO1 (C), *K. pneumoniae* (D), *A. baumannii* (E) and *S. aureus* JE2 (F) after 8 h incubation. Strains were grown in TSB:MES medium supplemented with 2 mM Ca(II) at 37 °C (mean ± SEM, n = 3). The indicated pH values correspond to the initial pH of the growth media. Data obtained at a 20 h timepoint are provided in Figure S6. The pH of the cultures after 8 and 20 h incubation is provided in Table S3.



**Figure 6.**

Analysis of Mn, Fe and Zn concentrations of MES:TSB medium treated with 250 µg/mL (10.4 µM) of CP-Ser at pH 5.0–7.0. The metal content of untreated medium (white bars), untreated medium after spin filtration (light gray bars), medium treated with CP-Ser (medium gray bars) and medium treated with CP-Ser in the presence of 2 mM Ca(II) (dark gray bars) was measured by ICP-MS (mean ± SEM, n = 4, \*P < 0.01). Complete metal analysis is provided in Figure S9 and Table S5. Metal analysis of MES:LB medium treated with CP-Ser is provided in Figure S10 and Table S6.

**Figure 7.**

(A) Analytical SEC chromatograms of CP-Ser (200  $\mu\text{M}$ ) in the apo ( $\alpha\beta$ ) form (black trace), in the presence of 10 equivalents Mn(II) (red trace), and in the Ca(II)-bound ( $\alpha_2\beta_2$ ) form (dashed black trace) (75 mM MES, 100 mM NaCl, pH 5.0–7.0) at 4  $^\circ\text{C}$ . Each chromatogram was normalized to a maximum absorbance of 1. Elution volumes are given in Table S7. (B–C) Mn retention by CP-Ser at pH 5.5–6.0 following SEC. Each plot contains a representative SEC chromatogram (red trace) and the quantification of protein and Mn concentrations in the collected fractions (bars).



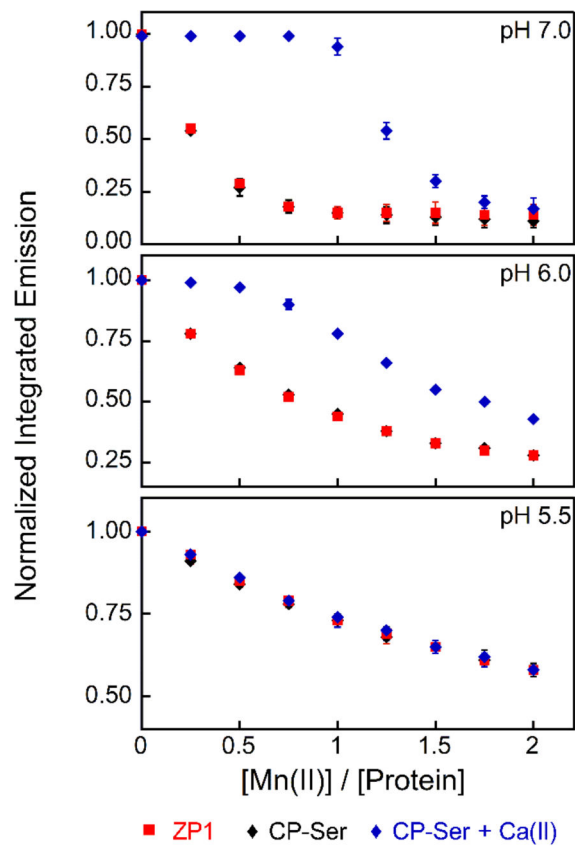


**Figure 8.** Mn(II) competition titrations between ZP1 (1  $\mu$ M) and CP-Ser (4  $\mu$ M) in the absence (black diamonds) and presence (blue diamonds) of 200  $\mu$ M Ca(II) at pH 5.5–7.0 (75 mM MES, 100 mM NaCl). All data are averages  $\pm$  SEM, n=3.

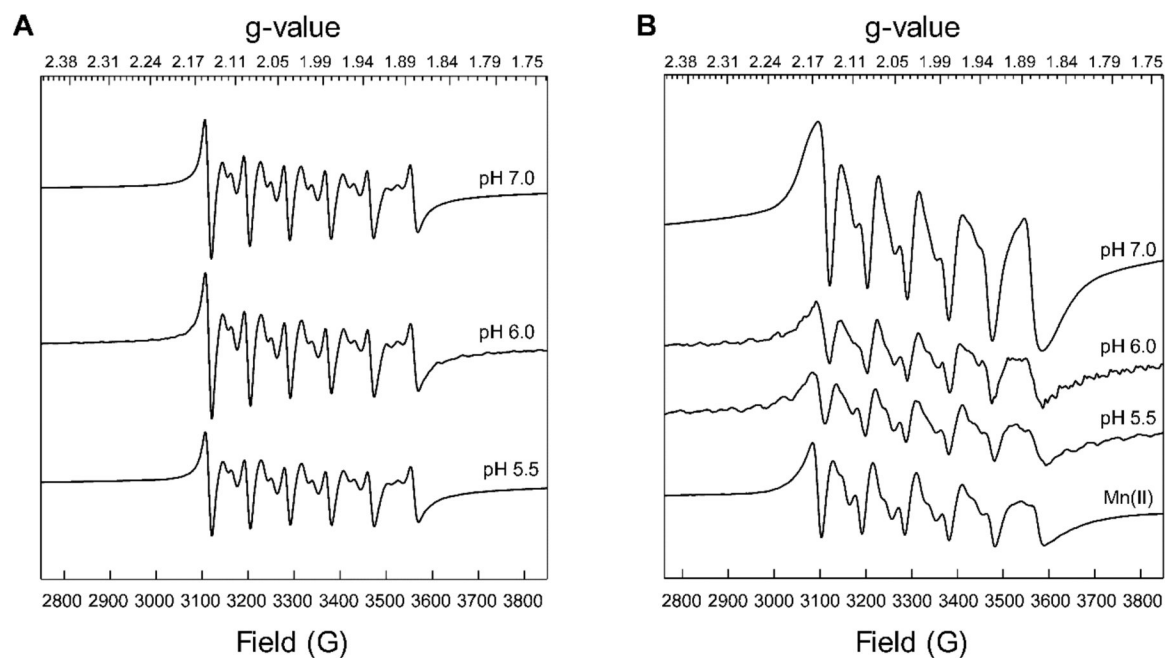


**Figure 9.** Low-temperature X-band CW EPR spectra of CP-Ser (200  $\mu$ M) incubated with 0.9 equivalents of Mn(II) at pH 5.5–7.0 (75 mM MES, 100 mM NaCl) in the presence (A) and absence (B) of 2 mM Ca(II). An EPR spectrum of Mn(II) (180  $\mu$ M) in MES buffer (75 mM MES, 100 mM NaCl, pH 5.5) is provided for comparison (panel B).

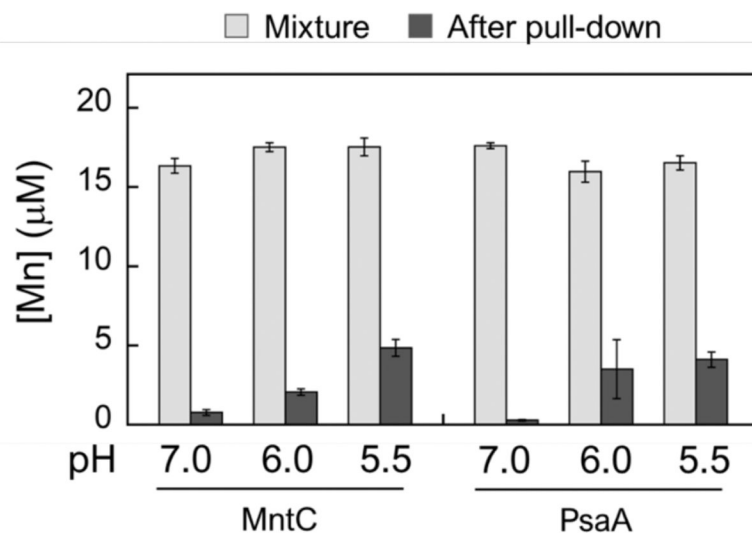


**Figure 10.** ICP-MS analysis of Mn(II) in solution before (light gray bars) and after (dark gray bars) pull-down of mixtures containing either MntC or PsaA (20 μM), B-CP (20 μM) and Mn(II) (18 μM) (75 mM MES, 100 mM NaCl, 1mM Ca(II), pH 5.5–7.0). The mixtures were incubated for 16 h at room temperature prior to pull-down with streptavidin resin. All data are averages ± SEM, n=3.